Environmental Fluid Mechanics **3:** 85–107, 2003.

Influence of Downstream Control and Limited Depth on Flow Hydrodynamics of Impinging Buoyant Jets

MURAT ULASIR[a] and STEVEN J. WRIGHT*
University of Michigan, Department of Civil and Environmental Engineering, Room 113 EWRE, 1351 Beal Ave. Ann Arbor, MI 48109-2125, USA ([a]E-mail: murat@engin.umich.edu)

Received 23 October 2001; accepted 3 July 2002

Abstract. Much study has been performed on the mixing properties of submerged, turbulent buoyant jets. It is safe to say that the problem of estimating dilution rates in vertical buoyant jets spreading in an 'infinitely deep' ambient water has been more than adequately resolved by previous researchers. However, the majority of environmental applications involve discharges into ambient waters of finite depths in which a bounding surface serves to re-direct the impinging buoyant jet horizontally into a radial spreading layer. Previous research indicates that this impinging jet undergoes additional mixing before buoyancy stabilizes vertical mixing and confines the spreading layer to the vicinity of the bounding surface. Unfortunately, the conceptualization and subsequent mathematical modeling of this additional mixing phenomenon is surrounded by considerable amount of disagreement between researchers. The purpose of this study is to provide, by means of velocity and concentration profile measurements, independent experimental evidence for the existence of a critical flow state immediately downstream of the active mixing zone in the horizontally flowing, radial flow that forms after impingement. It is further shown that this critical flow state must be expressed in terms of a composite Froude Number that takes into account the possibility of a non-zero exchange layer flow. Finally, the influence of the presence of a sill-like topographic downstream control on the criticality of the radial flow immediately downstream of the active mixing zone is also investigated.

Key words: buoyant jets, composite Froude Number, density jump, downstream control, impingement, non-zero exchange flow

1. Introduction

Much of society's waste, whether it be industrial waste or effluent flow from wastewater treatment plants, is discharged into receiving waters through a submerged outfall. The density of such discharges (at least in ocean disposals) is often less than that of the ambient water and therefore the induced buoyancy tends to rise the discharge up to the water surface. During this process, the turbulent, buoyant jet entrains large volumes of ambient fluid and hence causes significant amounts of dilution.

Any outfall diffuser design in the United States has to adhere to some design specifications laid out by legal requirements, set forth by regulatory authorities.

*Corresponding author, E-mail: sjwright@engin.umich.edu

These requirements usually entail the definition of a mixing zone and the specification of either a concentration limit or a dilution value that needs to be met within this zone. A mixing zone may be defined as a region which includes both the submerged, buoyant jet itself and the region where the rising buoyant jet impinges upon the free surface and begins to flow laterally away as a buoyant surface layer [1]. On average, the size of a mixing zone may extend between tens to hundreds of meters within the immediate vicinity of the source discharge.

Much study has been performed on the mixing properties of submerged, turbulent buoyant jets. It is safe to say that the problem of estimating dilution rates in vertical buoyant jets spreading in an 'infinitely deep' ambient water has been more than adequately resolved by previous researchers. However, the majority of environmental applications involve discharges into ambient waters of finite depths in which a bounding surface serves to re-direct the impinging buoyant jet horizontally into a radial spreading layer. This radial jet was found to undergo additional mixing [1–4] before buoyancy stabilizes vertical mixing and confines the spreading layer to the vicinity of the bounding surface. This is an important finding because determining the mechanisms contributing to this additional mixing and incorporating them into the design scheme of outfall diffusers may make the design much more economical.

Unfortunately, the conceptualization and subsequent mathematical modeling of this additional mixing phenomenon is surrounded by considerable amount of disagreement between researchers. Wright *et al.* [1], for example, proposed a density jump model they adapted from the work by Wilkinson and Wood [5]. The premise of this model is that, in the absence of any topographic downstream control, which is usually the case in ocean outfall discharges, the radially spreading, horizontal flow (after impingement) undergoes a rapid transition in layer thickness. During this process, it entrains ambient water, and eventually attains an internally critical flow state further downstream, which also marks the end of the active mixing zone. Wright *et al.* further argued that if the horizontal spreading layer thickness is not a small portion of the total ambient water depth, as was the case in Wilkinson and Wood's analysis, the criticality of the downstream flow must be expressed in form of a composite Froude Number (to be defined below) which takes into account the possibility of a non-zero exchange layer flow. Since Wright *et al.*'s experiments involved only concentration profile measurements at a fixed radial distance from the impingement location, they could not provide direct experimental evidence for the existence of a critical flow state immediately downstream of the active mixing zone.

Opposition to the reasoning of critical flow downstream of an active mixing zone was raised by MacLatchy and Lawrence [6]. In their experiments on vertical, buoyant jets impinging on the water surface, they observed that local, composite Froude Numbers calculated at different radial distances in the horizontally flowing spreading layer (after jet impingement) indicated a decrease with distance. But this decrease never proceeded to an internally critical flow state.

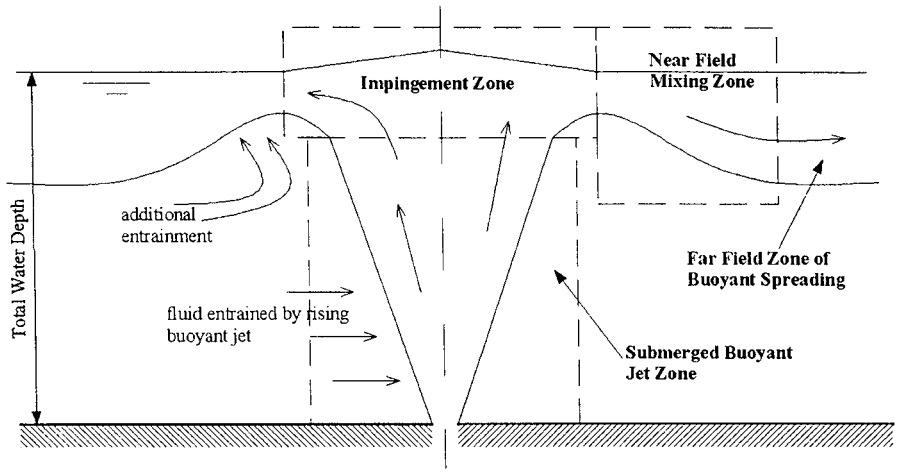

Figure 1. Definition sketch of submerged round buoyant jet impinging on a free surface.

The purpose of this study is to provide, by means of velocity and concentration profile measurements, independent experimental evidence for the existence of a critical flow state immediately downstream of the active mixing zone in the horizontally flowing, radial flow that forms after impingement. It is further shown that this critical flow state must be expressed in terms of a composite Froude Number that takes into account the possibility of a non-zero exchange layer flow. Finally, the influence of the presence of a sill-like topographic downstream control on the criticality of the radial flow immediately downstream of the active mixing zone is also investigated.

2. Background

In order to systematically analyze the problem of a vertically discharged buoyant jet impinging on a horizontal, bounding surface, we adopt a conceptual framework proposed by Tomasko [7]. According to this framework, the hydrodynamics of a buoyant jet can be conceptualized as consisting of four regimes, as indicated in Figure 1:
(1) The submerged buoyant jet zone in which the discharged fluid mixes with the ambient fluid by turbulent entrainment as it rises to the surface,
(2) the surface impingement zone within which the discharge reaches the ambient water surface and undergoes a vigorous transition whereby the flow changes direction from a vertical jet flow to a horizontally spreading surface flow along the ambient water surface, and
(3) the near field-mixing zone where the flow undergoes a rapid, turbulent change which results in further entrainment of ambient fluid,
(4) the far field zone of buoyant spreading where source characteristics of the jet become less important, rather, the conditions existing in the ambient surroundings

(such as ambient turbulence) control the trajectory and dilution of the buoyant jet through buoyant spreading and passive mixing [8].

At this point, it is important to realize that so long as the Bussinesq approximation of small density differences is applicable, the above stated flow zones are equally valid for positively buoyant jets impinging on a horizontal free surface and negatively buoyant jets impinging on a horizontal bottom. Wright *et al.* [1] showed that total entrainment rates are similar for both positively and negatively buoyant jets given the same discharge conditions.

Upon closer examination, the near field mixing zone in Figure 1 indicates a flow transition whereby the horizontally flowing surface layer of the buoyant jet undergoes a rapid transition in layer thickness. This transition is accompanied by additional entrainment in addition to the amount of entrainment the rising, vertical portion of the buoyant jet experiences. Many researchers investigated this transition, albeit under different experimental configurations. The flow in this zone has also been referred to by a number of different terms including wall jet, internal hydraulic jump, and density jump. Differences in definitions are generally related to the method for analysis of the phenomenon. The lack of a nomenclature (and the related issue of analytical approaches) that is universally agreed to has hampered discussion of results from previous studies. A brief summary of various definitions is provided in order to facilitate a discussion of the present experimental results.

The definition of a *wall jet* is generally accepted as a discharge from a confined source that experiences entrainment of fluid from the ambient into the discharged fluids. Analytical approaches for buoyant wall jets take an approach typified by that of Ellison and Turner [9] in which governing conservation equations for fluid mass, momentum and buoyancy are integrated through cross sections normal to the wall. This yields a set of parabolic ordinary differential equations that are solved as an initial value problem. Even though Ellison and Turner's model is for a dense discharge spreading on a bottom boundary, it should also remain generally valid for buoyant flows spreading along a free surface so long as the Bussinesq approximation of small density differences is satisfied. Two primary features of the aforementioned solution procedure are:

(1) The integrated fluid continuity equation requires the specification of an entrainment function that replaces the turbulence closure problem in the original partial differential equations and

(2) for buoyant flows, the equations predict a singularity downstream from the source for wall jets on horizontal walls as well as ones with small slope.

Ellison and Turner recast the integrated conservation equations into two equations determining the rate of change of the spreading layer thickness h and the Richardson Number, $\mathrm{Ri} = \mathrm{g}' \cdot \mathrm{h}/\mathrm{v}^2$ in which g' is the corrected gravitational acceleration term expressed as $\mathrm{g} \cdot (\Delta\rho/\rho)$) and v the spreading layer velocity. g is the gravitational acceleration term, $\Delta\rho$ is the density difference between the spreading layer and the ambient fluid and ρ is a reference density. This Richardson number is the inverse of internal Froude Numbers referred to below. The solution approach is

strictly valid only for discharges in which the initial Richardson number is less than a value of one. The singularity occurs at a Richardson number of one in Ellison and Turner's formulation if the profile constants in their formulation are set equal to unity. Not only does the singularity provide the inability to compute a solution for Richardson Numbers greater than one (Froude Numbers less than one) but the parabolic nature of the equations does not permit the occurrence of downstream phenomena such as topographic controls to be recognized in the solution procedure.

The phenomenon of a hydraulic jump in free surface open channel flow has been well established in literature. A hydraulic jump is analyzed by applying discrete continuity and momentum equations across the jump that is normally treated as a flow discontinuity although all hydraulic jumps have a discrete length [10]. Wall shear stresses (normally neglected in the formulation) and a weight component (in the case of a non-horizontal channel) terms require knowledge of the jump length in order to specify those terms in the momentum equation. The application of the continuity and momentum equations only allows for the downstream depth to be computed if the upstream depth is specified or vice versa. The process of computing the location of a hydraulic jump in a typical free surface flow application requires the computation of gradually varied flows both upstream and downstream of the jump location until a specific location within the channel is identified that locally satisfies the discrete continuity and momentum equations. Wall shear provides the mechanism by which depth variations occur that allows this condition to be satisfied at a unique location. However, the gradually varied flow equations are also parabolic and require initial conditions in order for the problem to be resolved. Thus, it is necessary to specify the flow state downstream from a specific upstream discharge in order to resolve the conditions through the jump.

An extension of the regular hydraulic jump concept in open channel flow is the notion of a jump-like flow transition at interfaces of two moving fluids of different densities. Hence the term *internal hydraulic jump*. The phenomenon of an internal hydraulic jump for two moving layers was perhaps first treated by Benton [11]. In his study, Benton defines critical flow as the velocity distribution relative to a coordinate system translated with an infinitesimal long wave. He indicates that the principles of momentum conservation and decrease of energy are together insufficient to specify downstream conditions of the 'internal jump', even when a complete description of the upstream flow is given.

By assuming no momentum transfer between layers, i.e. no interfacial shear stress and hence no mixing across the layers and hydrostatic pressure distribution across the jump, Yih and Guha [12] were able to solve the problem. Their approach requires the specification of discrete continuity and momentum equations in each of the two layers.A schematic of the flow configuration considered by Yih and Guha is given in Figure 2. Here, h_1 and h_2 are the initial layer thicknesses of the upper and lower layers respectively. q_1 and q_2 are the volumetric fluxes per unit

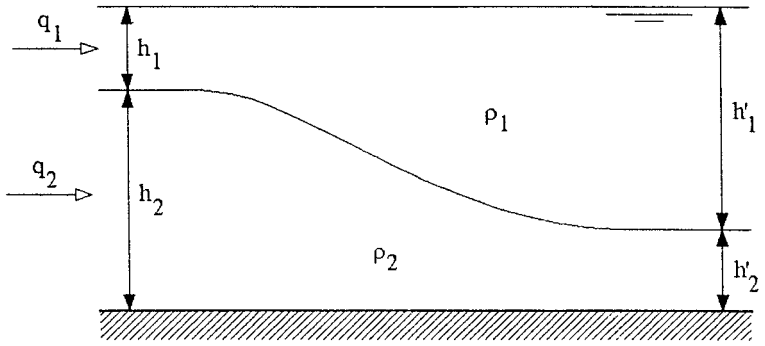

Figure 2. Schematic of a two layer exchange flow system adapted by Yih and Guha [12].

width, and ρ_1 and ρ_2 are the upper and lower layer densities respectively. h'_1 and h'_2 are the corresponding conjugate depths of the upper and lower layers.

Yih and Guha showed that if both layers are moving, up to three conjugate downstream states are possible for a given upstream flow condition. However, the downstream state cannot be determined by momentum and energy considerations alone. Thus, which of the three possible conjugate states will be realized after the jump depends on the type of downstream condition.

Another important result of their study is that if the densimetric Froude Number (Fr_i) of either layer is predominantly large, there exists only one conjugate state. The $(Fr_i)^2$ is defined as $q_i^2/(g' \cdot h_i^3)$ where $i = 1, 2$ and $g' = g \cdot (\rho_1 - \rho_2)/\rho_3$, g being the gravitational acceleration term.

Given the assumptions employed by Yih and Guha, under the particular circumstance where only a single layer is flowing, the resulting solution is similar to the ordinary hydraulic jump with the gravitation acceleration g replaced by the apparent gravity g' [13] thus providing an analogy between the ordinary and internal hydraulic jumps. However, for a given upstream state, the downstream state is uniquely determined irrespective of the possible presence of a downstream control such as a sill. In fact, Rajaratnam and Powley had to adjust a specific downstream control in order to produce a specific jump required to match their formulation, making the result not general. The dilemma can be resolved by adding an extra degree of freedom to the problem, namely allowing mixing between the two layers.

Wilkinson and Wood [5] approached the problem from a rather different perspective. They analyzed horizontal, two dimensional dense flow discharges in which the ambient layer depth was much greater than the dense layer thickness ($h/H \ll 1$), i.e., no flow of appreciable magnitude is assumed to take place in the upper layer. A schematic of their experimental setup is shown in Figure 3.

The discharged dense layer fluid was forced to undergo a rapid transition in layer thickness in a mixing region prior to where buoyancy stabilized the flow. Since such mixing resulted in a change in the density of the flowing, dense layer, the region of rapidly varied flow was referred to as a *density jump.*

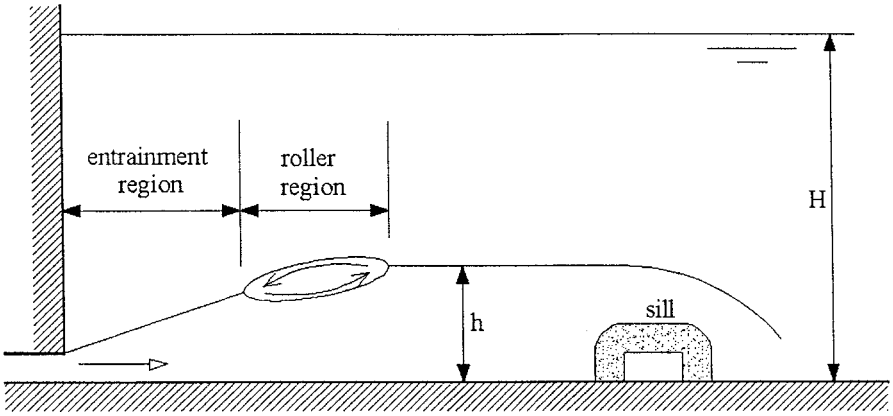

Figure 3. Schematic diagram of a density jump (from Wilkinson and Wood [5]).

Density jumps are similar in many ways to open channel hydraulic jumps. They are both transitions from a supercritical flow state to a subcritical flow state. One important difference between a density jump and an open channel hydraulic jump, Wilkinson and Wood argued, is the ability of a density jump to entrain varying amounts of ambient fluid necessary to satisfy a range of possible downstream controls. Even though an open channel hydraulic jump does entrain air, the immiscibility of the two fluids allows for the subsequent release of the air.

Wilkinson and Wood divided the density jump into two distinct regions, an entrainment region and a roller region. Nearly all the entrainment that occurs in the jump is said to take place in the entrainment region. The entrainment mechanism in this region was further argued to be similar to a neutral wall jet. The presence of a downstream control such as a sill is argued to cause a roller region to form at the downstream end of the jump. The roller region is characterized by a flow near the interface in the reverse direction to the main flow. This roller is reported to be similar in appearance to a roller associated with a submerged, open channel hydraulic jump.

Another important conclusion that came out of Wilkinson and Wood's study was that in the absence of any downstream control, the roller region in the density jump disappeared and the resulting density jump was of maximum entraining type. The flow downstream of the jump was observed to be critical in nature, i.e. the densimetric Froude Number of the dense layer was approximately equal to one.

The analysis of the density jump proceeds in a fashion similar to that for a conventional hydraulic jump. Discrete conservation equations for fluid momentum and buoyancy (due to the change in mass) are required to solve the problem. An important difference is that the equations are written over the entire depth rather than by layers as in the analysis by Yih and Guha. In addition, a downstream control condition related to the stratified flow at the weir or sill (or the downstream critical flow condition when no sill is present) is required to complete the analysis. It is important to notice that this unique approach accomplished two important goals:

(a) It was not necessary to define interfacial shear stress terms for the density jump, and
(b) this approach did not require the specification of a certain entrainment relationship, i.e., no entrainment function was required. The amount of entrainment into the jump could directly be calculated from momentum, continuity and buoyant flux conservation considerations.

Stefan and Hayakawa [14] performed experiments similar to Wilkinson and Wood's. They confirmed the findings by Wilkinson and Wood that entrainment and turbulent mixing occur only in the immediate vicinity of the point of discharge and that entrainment in this region is highly sensitive to changes in outlet or downstream conditions.

Chu and Baddour [15] extended Wilkinson and Wood's work to flow conditions where both layers are in motion, i.e., discharges into limited water depths. They realized that when turbulent entrainment is contributing to the exchange of momentum between those two layers, realistic assumptions on the forces that are active between the layers (such as shear forces) will no longer be possible. They wrote the momentum equations between the upstream and downstream portions of the density jump such that they extended over the entire flow depth.

Chu and Baddour further argued that in many practical applications, energy dissipation due to turbulence primarily occurs in one of the two layers. Under such a condition, energy flux can be assumed to be conserved in at least one of the layers, they argued. In other words, by using an energy conservation assumption in one of the flowing layers, Chu and Baddour were able to extend Wilkinson and Wood's work to cases where there is a flow in the upper layer.

It is possible to relate the various analyses discussed above, at least conceptually. It is necessary to recognize that supercritical miscible two layer flows will generally involve entrainment from one fluid layer to another and the amount of that entrainment depends on the specific downstream control. In fact, only by adjusting the downstream control to provide the condition desired were Rajaratnam and Powley able to obtain a non-mixing jump to satisfy the conditions of their analysis. The implication is that a downstream control must be considered in any supercritical two-layer mixing problem of limited depth. The problem can be analyzed as a density jump following the approach outlined by Wilkinson and Wood and extended by Chu and Baddour. It can also be described as a wall jet in order to account for the details within the entrainment region that generally would occur. The roller region described by Wilkinson and Wood can be thought of as an immiscible internal hydraulic jump of the sort analyzed by Yih and Guha that connects the wall jet with the subcritical two-layer flow forced by the downstream control. A consistent set of assumptions should provide equivalent predictions for total dilution in the mixing region using either analysis. The relative merits of each approach is the simplicity of the density jump model or the more detailed description of the mixing behavior of the wall jet/internal hydraulic jump description. Since the experimental results obtained in this study are presented within

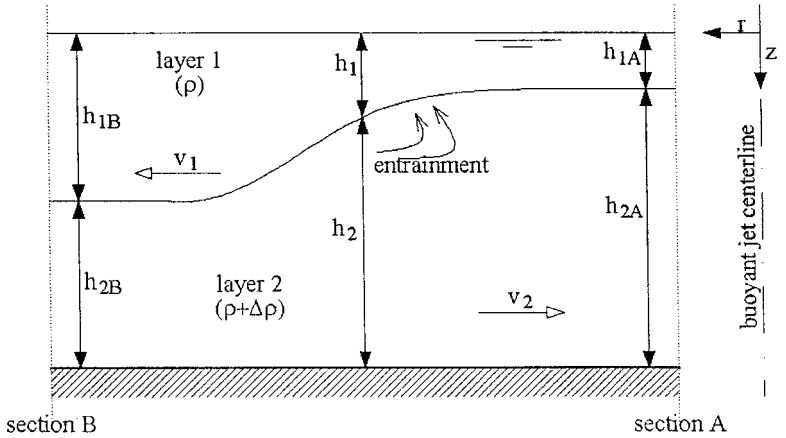

Figure 4. Schematic description of the near field mixing zone as a density jump.

the conceptual framework of a density jump, the subsequent section gives a brief introduction to the mathematical modeling aspect of a density jump.

3. The Density Jump Model

In this study, the near field mixing zone of the impinging buoyant jet (Figure 1) has been conceptualized as a density jump and the experimental results in this study are presented from this perspective. Thus, it is pertinent to give the reader a general understanding of the mathematical modeling principles involving the analysis of a density jump.

As mentioned in the background section, a general density jump analysis for a horizontal discharge utilizes the following equations (Chu and Baddour [15]):
(a) A momentum equation written over the entire depth of the two-layer system,
(b) a buoyancy conservation equation,
(c) a continuity equation that accounts for the mass exchange between layers,
(d) an energy conservation relation in the external layer, and
(e) a downstream control relation.

Figure 4 gives a schematic description of a density jump. In this figure, section A marks the end of the impingement zone, hence the beginning of the near field mixing zone. This zone extends all the way to section B after which buoyancy forces stabilize the flow and confine it to the vicinity of the bounding surface. h_1, h_2, v_1, and v_2, refer to local layer thickness and velocity terms in the respective layers at an arbitrary radial distance from the vertical, buoyant jet axis.

The downstream control relation specifically expresses the conditions in the two-layer flow downstream from the end of the density jump (section B in Figure 4). For example, in the case of a sill of sufficient height located downstream of the jump, the control relation requires the assumption of internally critical flow at the sill as well as energy conservation to define the subcritical flow state upstream

of the sill and controlled by the critical flow at the sill [5]. Essentially, the exchange flow at the sill dictates the amount of mixing that can occur within the density jump and controls the size of the roller region.

In the absence of a specific topographic control, Wilkinson and Wood determined that the entrainment into the density jump proceeded until it reached a maximum. This condition was also accompanied by an internally critical flow state immediately downstream of the density jump (section B in Figure 4). Under this condition the occurrence of critical flow serves as the necessary downstream control relation.

When the water depth is large with respect to the later thickness, the dynamics of the lower layer in Figure 4 (h_{2B}) are unimportant and the critical flow condition at section B can be expressed as $Fr_{1B}^2 = 1$, where $Fr_{1B}^2 = v_{1B}/\sqrt{g'_B \cdot h_{1B}}$. Here, v_{1B} is an average velocity in layer one, section B, h_{1B} is an average layer thickness, and $g'_B = g \cdot (\Delta\rho/\rho)_B$, where g is the gravitational acceleration term and $(\Delta\rho/\rho)_B$ is the normalized density difference at section B.

In the case of limited depth, however, the flow in the upper layer becomes non-negligible and the upper layer dynamics must be accounted for in the momentum equation, the external layer energy conservation relation and the downstream control expression.

Critical flow relations for two-layer flows can be derived in a number of ways [16, 17]. One of the most instructive ways is to consider the speed of propagation of long internal waves. Schijf and Schönfeld [18] derive a relation for internal wave speeds for two layer flows. While a number of explicit assumptions are required in their analysis, the resulting expression for internal wave propagation for a two-dimensional flow system is:

$$c_i = \overbrace{\frac{v_1 \cdot h_2 + v_2 \cdot h_1}{H}}^{\text{I}} \pm \overbrace{\sqrt{\frac{\Delta\rho}{\rho}\, g\, \frac{h_1 \cdot h_2}{H} - \frac{(v_2 - v_1)^2\, h_1\, h_2}{H^2}}}^{\text{II}}, \tag{1}$$

where H is the total water depth and the rest of the terms are referred to local variables as indicated in Figure 4. (c_i) is the propagation velocity of long internal waves as measured by a stationary observer. The first term in Equation (1), i.e., (I) is termed the 'convective velocity'.

In order to determine the direction of wave propagation with regards to a reference point, here and in the ensuing discussion, upstream is defined in the opposite direction of the 'convective velocity', namely, if the convective velocity is positive in the flow arrangement given in Figure 4, then upstream is in the opposite direction to the velocity vector in layer 1 (this is the dominant layer because the 'convective velocity' is greater than zero).

In order for Equation (1) to produce only positive roots for (I) > 0 (positive convective velocity), namely, if we wish the upstream propagation of waves to be

blocked, then (I) $\geqslant$ (II). It can easily be shown that this condition is analogous to the following statement:

$$\frac{v_1^2}{\frac{\Delta\rho}{\rho} g h_1} + \frac{v_2^2}{\frac{\Delta\rho}{\rho} g h_2} = Fr_1^2 + Fr_2^2 \geq 1, \tag{2}$$

where the condition of $Fr_1^2 + Fr_2^2 = 1$ represents a critical flow state in which the upstream propagating disturbance is stationary. In other words, if the sum of the Froude numbers over the entire water depth (*the composite Froude Number*) is greater than or equal to one, no wave can propagate upstream.

In the limiting case where $h_1 \ll h_2$ and $v_1 \gg v_2$, the critical flow condition expressed with Equation (2) reduces to $F_1^2 = 1$. This condition is referred to as the 'great depth case'. Consider what happens if the discharge conditions are held fixed while the total water depth H is gradually reduced. The following flow regimes can be identified:

(1) As the depth is decreased below the great depth limit, the velocity in layer 2 becomes important and the exchange flow is reduced due to the contribution to F_2. Initially however, this contribution is small and the major effect is simply a reduction in entrainment in the density jump.

(2) A further decrease in depth results in a switch in sign in the convective velocity across the density jump. At the upstream end of the jump (section A), the convective velocity is positive in the direction of v_1. However, on the downstream side of the jump (section B), the large value for h_{1B} and the high velocity in layer 2 results in a change in direction in convective velocity across the jump. We interpret this to imply that the upstream (in the sense of v_1) propagation of disturbances is no longer blocked in the downstream portion of the jump. In the context of the density jump, it is presumed that the entrainment occurs into a primary layer from a secondary layer and that the primary layer is defined on the basis of a positive convective velocity. Therefore, entrainment goes into layer 1 over the upstream portion of the density jump, but into layer 2 beyond where the convective velocity changes sign. This implies a recirculation region at the interface. Consistent with this would be a 'roller' that is induced by the limited depth as opposed to Wilkinson and Wood's sill-induced roller. The consequence of this depth induced roller would be a further reduction in dilution.

(3) Eventually, as the total water depth is reduced further, the layer thickness h_1 approaches the water depth. This type of flow has been termed an unstable near field by Jirka and Harleman [19].

Even though in an unstable near field configuration the layer thickness approaches the depth, entrainment does not cease although it must be constrained by the depth limitation. It is not clear at present what controls the exchange flow in this unstable near field configuration, but the density jump analysis is no longer applicable since the conditions immediately downstream of the jump cannot satisfy the two-layer approximation and velocities in both directions are required near

the surface. Visual observations by Wright [2] indicate that in a two dimensional channel with dense bottom discharge, a portion of the surface flow moves upstream while another portion moves in the opposite direction. For radial flows, Wright *et al.* [1] observed that the radial symmetry of the flow was lost and outflow occurred over a portion of the circumference while inflow occurred over the entire depth through the remaining portion.

It was noted above that the density jump analysis breaks down in the limit of the unstable near field since the conditions downstream of the jump cannot be described with a two-layer approximation. However, it is probable that there is an even more restrictive constraint on the general analysis, specifically with regards to the energy conservation argument in the upper layer. Once the depth induced roller region is produced, layer 2 looks like the entraining layer to the flow at the downstream side of the density jump. Since the entraining layer does not conserve energy, it appears that a different relation is necessary to close the system of equations.

4. Scaling of Flow

The characteristics of a round, turbulent buoyant jet, such as its near field dilution (amount of dilution the buoyant jet experiences as it rises vertically toward a bounding surface), may be assumed to be a function of its source conditions, which may be described uniquely by Q (the source volumetric flux), B (the source buoyancy flux), and M (the source momentum flux), as well as the axial distance z from the nozzle. Here $Q = v_o \pi D^2/4$ where v_o is the nozzle discharge velocity and D is the nozzle diameter, $B = g \cdot \Delta\rho_o/\rho \cdot Q$ or $B = g'_o \cdot Q$ where g is the gravitational acceleration term, g'_o is the corrected gravitational acceleration term, $(\Delta\rho)_o$ is the density difference between the discharge fluid and the ambient fluid, and $M = v_o^2 \pi D^2/4$.

Dimensional analysis yields two independent length scales, namely: l_Q $(= Q/M^{1/2})$ and l_M $(= M^{3/4}/B^{1/2})$. The physical significance of l_Q is that it indicates the length over which source conditions (such as the geometry of the jet nozzle) are important in the mixing of the jet [20]. The momentum length scale l_M, on the other hand, is a measure of the distance beyond which the effects of the initial momentum flux become negligible. In other words, beyond this distance a buoyant jet starts behaving like a pure plume. Usually l_Q is smaller than l_M. So, within the perspective of this analysis, as a less dense buoyant jet, for example, rises toward the surface of ambient water of depth H, it undergoes the following transitions:

(1) At a distance $z \ll l_Q$, the flow is influenced by its initial momentum and discharge fluxes,

(2) between a distance $l_Q \ll z \ll l_M$, the flow behaves like a pure jet because flow parameters (such as jet center line velocity and jet spreading width) are predominantly controlled by M, and finally

(3) at a distance $z \gg (l_M, l_Q)$, since the behavior of flow parameters are determined mainly by B, it behaves like a pure plume.

Scaling relations of the type discussed above can also be used to determine a functional form for the total rate of entrainment into buoyant jets impinging on a bounding surface. For example, if the total water depth H into which the buoyant jet is released is much larger than the momentum length scale l_M, then the total volumetric flux q at the end of the near field mixing zone must be controlled by the parameters B and H only. It is also assumed that the zone of flow establishment is much smaller than the total water depth, i.e., $H \gg l_Q$. As a consequence, $q \sim B^{1/3}H^{5/3}$. If S_{avg} is defined as q/Q, Q being the source volumetric flux, the following relation must hold true for the total amount of dilution at the end of the near field mixing region:

$$\frac{S_{avg}Q}{B^{1/3}H^{5/3}} = \text{constant}. \tag{3}$$

A functional form for the thickness of the spreading layer at the end of the near field mixing region, too, can be determined, namely, that $h/H = \text{constant}$, this being the only dimensionally consistent result. This result is also applicable to any other dimension of the 'surface jet'/'near field mixing zone' (such as the radius of the density jump) so long as there is no downstream control acting on the spreading layer.

The dilution problem becomes more complicated when the source momentum flux 'M' begins to play a more dominant role in the mixing process. In this case, Equation (3) can be shown to take the following form:

$$S^* = \frac{S_{avg}Q}{B^{1/3}H^{5/3}} = f\left(\frac{l_M}{H}\right), \tag{4}$$

where S^* is termed the normalized average dilution at the end of the near field mixing zone (density jump zone). The same would be valid for the spreading layer thickness, i.e., $h/H = g(l_M/H)$. The functional form in equation (4) can only be determined with the help of either experimental data or additional considerations beyond dimensional analysis.

5. Experimental Procedure

The experimental setup in this study entails a negatively buoyant jet discharging into a large tank filled with ambient water, impinging upon a horizontal, submerged bounding surface, spreading radially on it, and eventually leaving the bounding surface by flowing over its edge and falling to the bottom of the experimental tank. The size of the tank is 13.7 m $\times$ 4.6 m with a total depth of 2 m. The top and side views of the experimental tank are shown in Figure 5. A false bottom with a diameter D of 3 m was placed within the tank. For some experiments, a plate

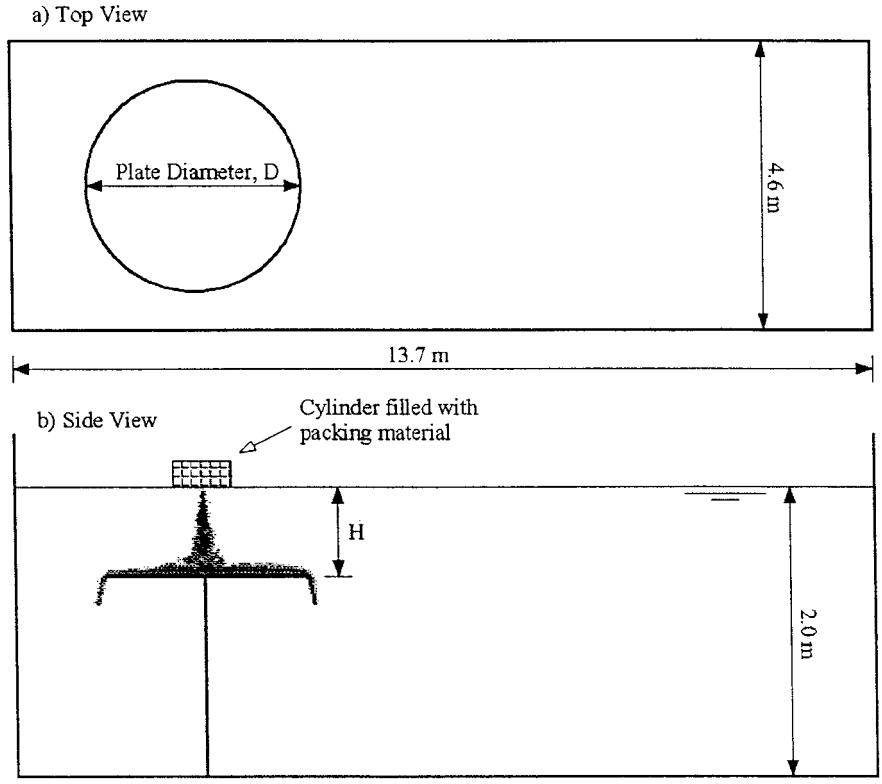

Figure 5. Dimensions of the experimental tank, top and side views.

with a diameter of 1.5 m was utilized. The submergence height H of the plate from the water surface (free surface) was varied between 15 cm to 45 cm throughout the experimentation. Such an experimental configuration enabled us to perform the experiments for an extended period of time without worrying about salt water backup. This way, several profile measurements at various radial distances could be made. Also, letting the buoyant jet impinge on a submerged plate and have it fall off its edge created a very specific downstream control, namely a critical flow condition at the edge of the plate.

Salt water solutions prepared in a large mixing tank were first pumped into a constant pressure tank. Later, the salt water solution was discharged into the experimental tank filled with fresh water. During this process, the salt water was first passed through a flowmeter and then through a small cylinder before it was released into the experimental tank through an orifice opening located at the bottom of this cylinder. The small cylinder was filled with packing material in order to straighten the flow before it was discharged into the experimental tank. At the bottom of the cylinder was an opening that was covered with an orifice plate. The size of the orifices varied from 0.2 cm to 0.5 cm. This arrangement ensured that the discharge flow had a top-hat velocity profile right at the onset. Due to the flow contracting at

the sharp edged orifice plates, a flow contraction coefficient of 0.63 was applied to the flow area.

The velocity data was obtained with a MicroADV manufactured by Sontek, Inc. The salt water concentrations were measured using a conductivity probe. Before each experimental run, it was ensured that the discharge solution and the ambient water were at the same temperature.

The data gathering process involved the usage of an appropriate sampling frequency and time. These were determined by means of amplitude spectrum and autocorrelation function analyses. After conducting several experiments with a wide range of initial conditions, it was found that a sampling frequency of 2 Hz and a total sampling time of 240 s (4 min) provided a statistical convergence of both the velocity and conductivity data to within approximately 5%. This convergence worsened as the radial distance for gathering data increased. However, within the near field mixing zone of a wide variety of initial conditions, the above stated convergence error was observed to hold. Details about the analysis leading to the above mentioned sampling frequency and time can be found in reference [21].

5.1. CALCULATING AVERAGE QUANTITIES

The local point velocity and conductivity measurements taken during the experimentation need to be converted to average layer properties at different radial distances in order to interpret the hydrodynamic flow behavior of the flow as a whole. The conversion was done in the following manner:
(a) The layer velocity and thickness of the dense layer (layer 1) was calculated using the first and second moment of the radial velocity distribution, i.e.,

$$v_1 \cdot h_1 = \int_0^{h_n} v \cdot dz \tag{5}$$

and

$$v_1^2 \cdot h_1 = \int_0^{h_n} v^2 \cdot dz, \tag{6}$$

where h_n is the vertical distance from the submerged, horizontal plate at which the radial velocity changes direction. Also, (v_1) and (h_1) are the layer velocity and thickness respectively of layer one. (v) represents local velocity. Since in the actual measurements, local values were measured at discrete intervals, the integral equations shown above need to be converted to summations. This was done in the following manner.

$$v_1 \cdot h_1 = \frac{(z(1) + z(2))}{2} \cdot v_{z(1)} + \sum_{i=3}^{n} \frac{(z(i) - z(i-2))}{2} \cdot v_{z(i-1)}, \tag{7}$$

where z(i) is the vertical distance from the plate surface and $v_{z(i)}$ is the local point velocity. n is the point corresponding to where z is approximately equal to h_n. The first term on the right side of the equal sign in Equation (7) was necessary because the lowest z, i.e., z(1) was on the order of 0.5 cm and not zero. Such a formulation was assumed to take properly into account the flow features at vertical distances below z(1). This was particularly important when local buoyancy flux terms were calculated because the g' value very close to the plate surface accounted for a significant portion of the overall, local buoyancy flux.

The summation form of Equation (6) is very similar to Equation (7) and is not shown here.

(b) the average corrected gravitational acceleration term (g') in layer one was calculated using local buoyancy and discharge flux terms, i.e.,

$$g'_1 = g \cdot \left(\frac{\Delta\rho}{\rho}\right)_{avg} = \frac{\int_0^H g\,\frac{\Delta\rho}{\rho}\,v\,(2\pi r)\,dz}{\int_0^H v\,(2\pi r)\,dz} = \frac{\beta}{q}, \tag{8}$$

where ($\Delta\rho$) is the density difference between the dense jet fluid and the ambient water. (ρ) represents the density of the ambient water. (β) and (q) are local buoyancy and volumetric fluxes respectively.

The discrete (summation) form of the local buoyancy flux was expressed as

$$\beta = 2 \cdot \pi \cdot r \cdot \left[g'_{z(1)} \cdot v_{z(1)} \cdot \frac{z(1) + z(2)}{2} + \sum_{i=3}^{m} g'_{z(i-1)} \cdot v_{z(i-1)} \cdot \frac{z(i) + z(i-2)}{2} \right], \tag{9}$$

where r is the radial distance from the jet center line to where vertical, cross sectional layer properties are determined. $g'_{z(i)}$ is the local, point gravitational acceleration measurement and m is the point which corresponds to the vertical distance from the plate surface for which $g'_{z(i)}$ is zero.

The local volumetric flux was then inferred from layer properties as follows:

$$q = 2 \cdot \pi \cdot r \cdot h_1 \cdot v_1. \tag{10}$$

5.2. DETERMINING THE DIAMETER OF THE IMPINGEMENT SURFACE

The diameter of the submerged plate was carefully chosen as well. It was sufficiently large to fully contain the near field mixing zone and at the same time small enough to minimize viscous effects.

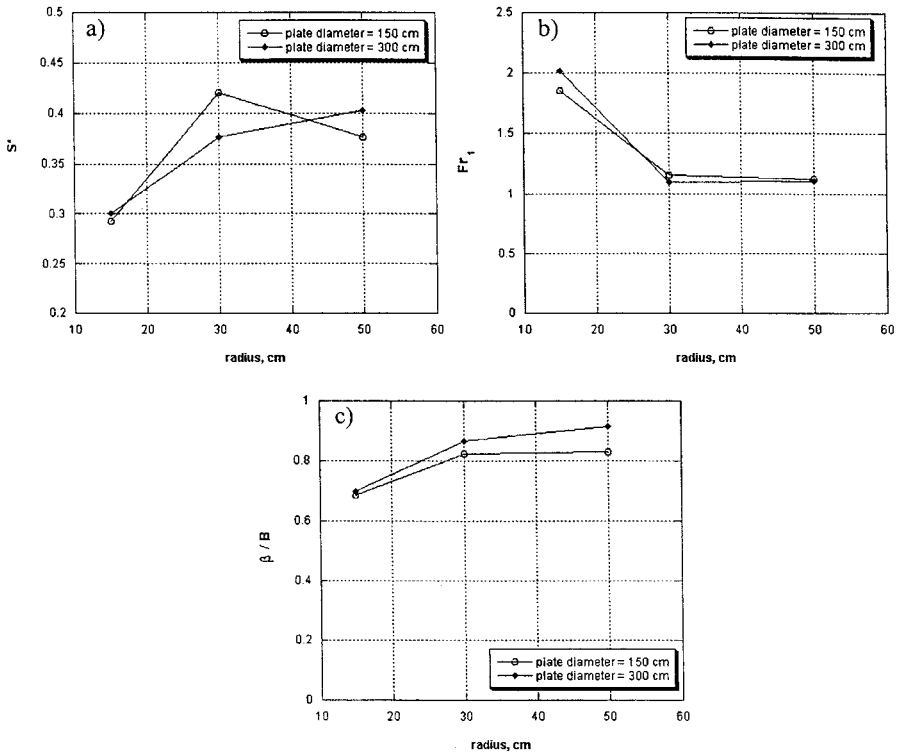

Figure 6. Comparing (a) S^*, (b) Fr_1, and (c) buoyancy flux ratios at different radial distances for experiments conducted using different plate sizes. Discharged condition is $l_M/H \approx 0.23$.

Figure 6 compares (S^*), Froude Number (Fr_1), and (β/B) values for an initial discharge configuration of $l_M/H = 0.23$ at different radial distances and two different plate sizes. The layer 2 densimetric Froude Number is not computed, first of all because no data was gathered in the this layer and secondly, its effect on the overall composite Froude Number should be negligible. This assumption is true except for a few cases to be discussed further below. The reason that no data was gathered in the second layer is because the ADV signal to noise ratio in the fresh water (second layer) was unacceptably high for the purposes of this study.

It is obvious from these plots that even average flow properties do not show a dependence on the size of the plates utilized in the experiments. Further details about the effects of plate size on the flow properties of the impinging buoyant jet can be found in [21].

6. Results

This section summarizes results of experimental studies with regard to the influence of a downstream weir and the change in total water depth on the amount of entrainment into the near field mixing zone of the impinging buoyant jet.

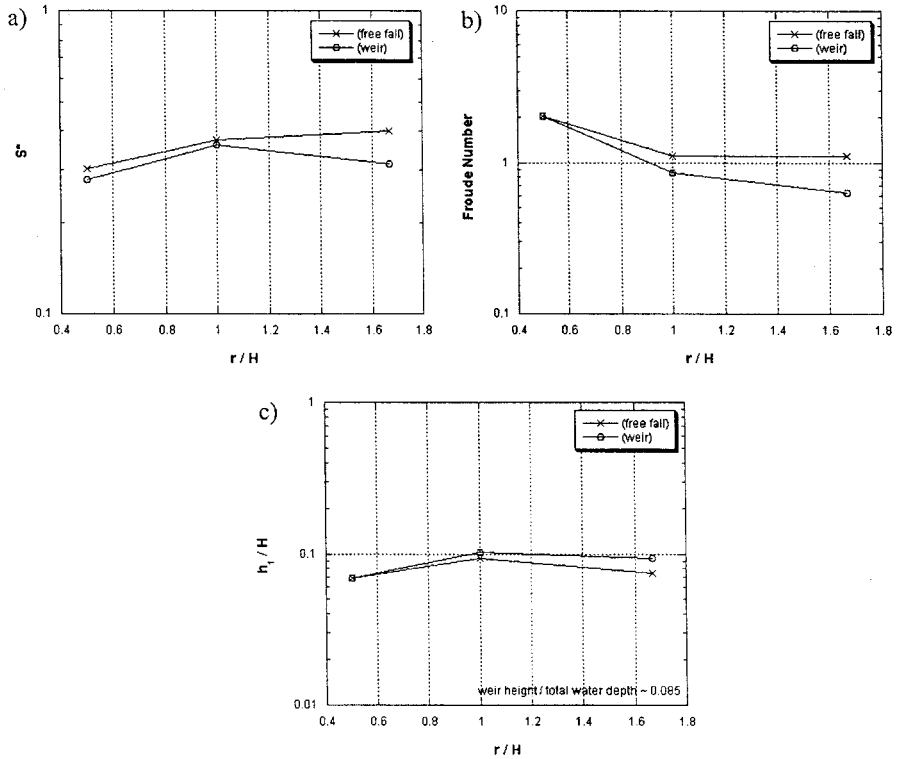

Figure 7. Influence of a weir of 2.54 cm height placed around the outside rim of the submerged plate on the flow conditions of radial jet. The (free fall) data represents conditions in which radial flow is allowed to fall freely of the end of the submerged plate.

6.1. INFLUENCE OF DOWNSTREAM WEIR ON FLOW CONDITIONS

It was mentioned earlier that Wilkinson and Wood [5] conducted experiments on two dimensional slot discharges. Their experiments indicated that entrainment into a vertically flowing dense layer jet was impeded by the presence of a sill placed downstream of the mixing region. In this study, this condition was tested by placing a weir of one inch (2.54 cm) height around the outer rim of the 150 cm diameter plate. The initial discharge condition was $l_M/H = 0.23$. Figure 7 clearly indicates that, as predicted by Wilkinson and Wood for two dimensional flows, the radial spreading flow does get influenced by the presence of an obstacle downstream of the mixing region. The horizontal axis in this figure is non-dimensionalized by the total water depth (H), which also corresponds to the vertical distance from the discharge nozzle to the surface of the submerged plate. The reason for a decrease in S^* in the case when a weir is placed downstream of the flow is that, as Wilkinson and Wood argued, the downstream obstacle creates a roller region which impedes entrainment of fluid from the upper layer into the laterally spreading dense layer.

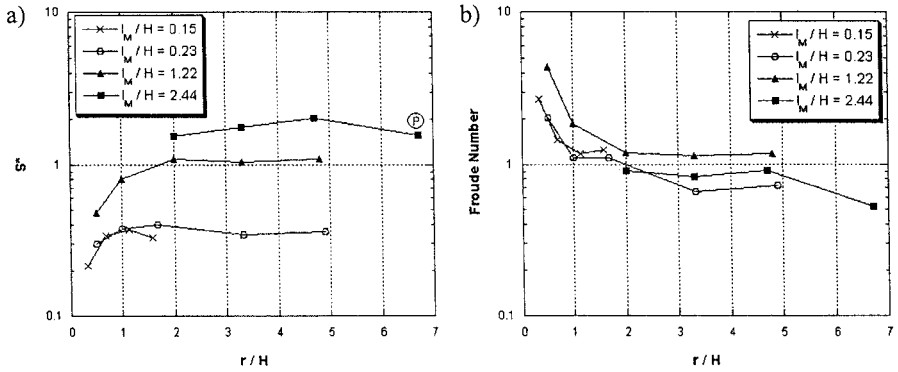

Figure 8. Flow conditions at the end of the near field mixing zone for different initial discharge configurations.

This phenomenon is also depicted in the graph showing the variation of the layer thickness (h_1) with radial distance (r). Even though the layer thickness at the end of the mixing region (where S^* does not increase anymore with r) is approximately the same as for the 'free fall' case, the non-dimensionalized dilution S^* is not. Furthermore, the 'backing up' of the flow with a downstream weir is also evidenced in Figure 7b as a decrease in Froude Number to below unity.

6.2. CRITICAL FLOW STATE AT THE END OF THE NEAR FIELD MIXING ZONE

As a vertical buoyant jet impinges upon a bounding surface and gets re-directed into a horizontal radial flow, intense mixing occurs in the near field mixing zone. After this zone, buoyancy forces stabilize the flow and confine it to a radial spreading layer at the vicinity of the bounding surface. This latter flow configuration is called the far field zone of buoyant spreading (Figure 1). In this zone, there is no additional mixing into the spreading layer.

Figure 8 summarizes flow conditions for different initial discharge configurations. Figure 8a indicates that, after a certain radial distance, the non-dimensionalized entrainment (S^*) into the radial jet ceases. Furthermore, this 'entrainment distance' seems to increase with l_M/H.

It is worth mentioning that the point marked as Ⓟ in Figure 8a is not a result of experimental error but rather a result of limited number of profile points gathered at that radial location. For example, there was no data gathered between local, vertical distances of 1.77 and 4.27 cm away from the surface of the submerged plate. Non-dimensionalized velocity plots presented later in this chapter indicate that this flow ($l_M/H = 2.44$) must reach a maximum velocity at a local, vertical distance of approximately 3 cm. In order to assess the importance of this missing data point, consistent values for g' and local velocity were estimated based on non-dimensional velocity plots (mentioned later) and a trendline equation fit through g' values at this radial distance. As a result, a velocity of 0.55 cm/s and a g' of

0.18 cm/s^2 was assigned to a vertical distance of 3 cm. This data point increased local volumetric flux calculations by 23% and local buoyancy flux calculations by 8%. This was adequate enough to increase the S^* value at that radial distance from $\sim$1.6 (Figure 8a) to approximately 2.

Figure 8b shows that the overall layer 1 densimetric Froude Number (Fr_1) is much higher than one in regions where the flow entrains fluid from the upper layer. However, this number decreases to approximately one about where entrainment ceases and remains at that value. This trend seems to be less obvious for the case for which $l_M/H = 2.44$. Figure 8a, for example, indicates that entrainment for this initial flow configuration stops at a distance of approximately $5 \cdot r/H$. However, Froude Numbers for this configuration (Figure 8b) reach one at a distance of $2 \cdot r/H$ and remain that way.

One reason for this may be explained with regards to discussions presented earlier, namely that for this case, the ambient flow layer (layer 2) may have become dynamically active, i.e., the average velocity in this layer is no longer negligible and its contribution to the overall criticality of the exchange flow must be taken into consideration. Experimental data indicates, for example, that the maximum height for which g' becomes zero is approximately 54% of the total water depth H for this experiment. Thus, the hydraulic conditions of the upper layer must be taken into account. In this study, no direct velocity measurements were made in layer 2. As a consequence, there is no direct way to determine the Froude Number in this layer.

6.3. INFLUENCE OF TOTAL WATER DEPTH ON THE FLOW CONDITIONS AT THE END OF THE NEAR FIELD MIXING ZONE

In order to test the influence of total water depth on flow properties of the impinging buoyant jet, two discharge configurations were investigated. In one configuration l_M/H was equal to 0.23 with a total water depth (H) of 30 cm. In another, l_M/H was equal to 6.51 with a total water depth of 15 cm. The latter produced an unstable flow regime, meaning that the depth of the radial jet extended all the way to the water surface. The significance of this unstable near field flow regime was that it was 'just' unstable. Then, the total water depth (H) was raised by approximately another 15 cm, keeping the discharge nozzle suspended inside the water column with the same distance between the discharge orifice and the submerged plate surface (Figure 9). The same was done for the first discharge condition, even though the first case did not produce an unstable flow regime.

The reason behind creating an unstable flow regime and then increasing the submergence height was to create a condition in which the counter flowing ambient water layer became 'dynamically active' since the radial jet was forced to occupy a significant portion of the total water depth. Results from this experimental setup are rather interesting. Figure 10 provides results for the experimental configurations outlined above. For a flow condition which is represented by initial discharge

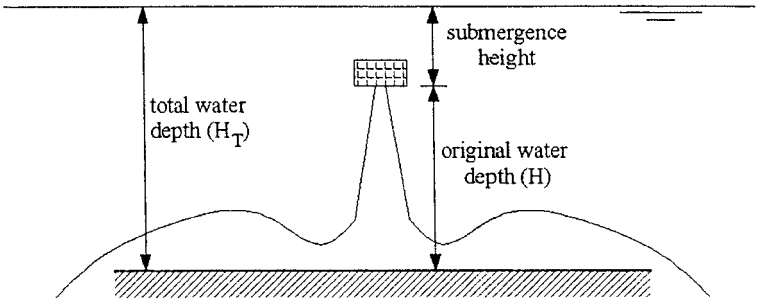

Figure 9. Total water depth compared to submergence height.

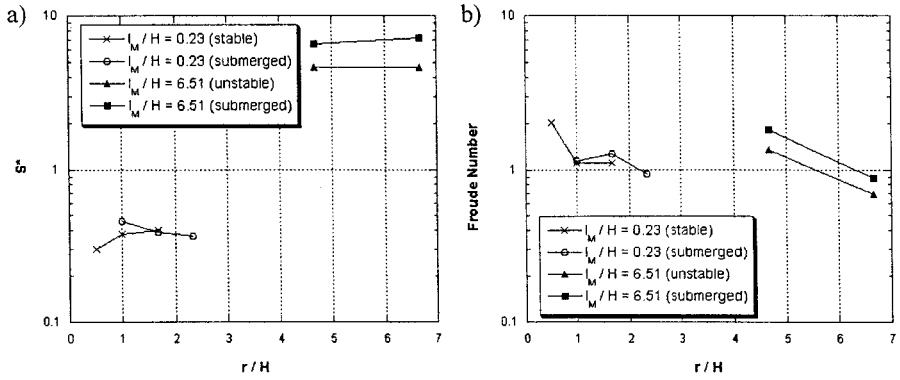

Figure 10. Influence of total water depth on a) the non-dimensionalized dilution (S*) and b) the lower layer Froude Number for different initial flow conditions.

conditions of $l_M/H = 0.23$, the ratio of the average, dense layer thickness (h_1) to the total water depth (H_T, Figure 9) was approximately equal to 0.07 at a radial distance of 30 cm from the buoyant jet center line. The ratio between the distance from the plate surface where the density reached the ambient water density to (h_1) was equal to 1.5. On the other hand, (h_1/H_T) was equal to 0.30 for the case of $l_M/H = 6.51$ at a radial distance of 70 cm. At the same radial distance, the ratio of the distance where the density reached zero to (h_1) was approximately equal to 1.6.

It is obvious from Figure 10 that the total water depth has a great influence on the hydraulic conditions of the dense layer flow, provided that the thickness of this layer is significant enough to cause a 'dynamically active' upper layer. The re-circulation region for the unstable flow condition ($l_M/H = 6.5$) extended to about (5 to 6) · H (in terms of radial distance from the jet center line of the buoyant jet).

7. Conclusions

Results of this study show that in the absence of any topographic downstream control, the horizontally moving radial flow (after impingement) attains a critical

state of maximum entraining type. For plume like discharges (corresponding to a momentum length scale l_M/H of less than 0.2) this critical flow condition can be expressed as the spreading layer densimetric Froude Number being equal to one. The average spreading layer thickness (h) in such flows is usually much less than the total water depth (H). Thus, such flow cases correspond to what is called a 'great depth solution' in the literature.

As source momentum is increased or the total water depth decreased, both of which imply a larger l_M/H, the counter-flowing ambient layer eventually becomes important. For no downstream control, this situation arises for an l_M/H of greater than approximately 2.5. In this case, the criticality of the downstream flow after the near field mixing zone must take into account the existence of a non-zero, ambient exchange flow. In fact, experiments conducted with a high l_M/H in which the spreading layer flow was initially 'just unstable' showed that as the total water depth was increased, namely a 'dynamically active' ambient exchange layer was formed, the densimetric Froude Number of the spreading layer flow adjacent to the near field mixing zone was not equal to one, again, confirming the belief that the dynamics of the ambient exchange flow must be considered in expressing the criticality of the downstream flow.

The importance of a downstream control on the flow properties of the spreading layer was also demonstrated with an experiment in which a weir was placed at the outer rim of the desk the buoyant jet impinged upon. The effect of this weir was to decrease the amount of dilution the spreading layer experienced compared to a 'free fall' case. This result further confirmed the initial proposition by Wilkinson and Wood that the effect of a downstream weir is to create a roller region that impedes entrainment into the spreading layer.

In conclusion, the total rate entrainment into the near field mixing zone of an impinging, buoyant jet is strongly influenced by the presence of a downstream control. In the absence of any downstream control, the flow attains a critical flow state of maximum entraining type. This condition can be expressed as the sum of the upper and lower densimetric Froude Numbers being approximately equal to one, i.e., $Fr_1^2 + Fr_2^2 \approx 1$.

References

1. Wright, S.J., Roberts, P.J.W., Zhongmin, Y. and Bradley, N.E.: 1991, Surface dilution of round submerged buoyant jets, *J. Hydraul. Res.* **29**, 67–89.
2. Wright, S.J.: 1986, *Aspects of Far Field Control on Buoyant Jet Mixing*, Institut für Hydromechanic und Wasserwirtschaft, ETH, Zürich, Switzerland, Report Number R24–86.
3. Roberts, P.J.W., Adrian, F. and Daviero, G.: 1997, Mixing in inclined dense jets, *J. Hydr. Eng.* **123**, 693–699.
4. MacLatchy, M. and Lawrence, G.: 1999, Radially spreading surface flow. In: *Proceedings, International Symposium on Environmental Hydraulics*, Hong Kong.
5. Wilkinson, D.L. and Wood, I.R.: 1971, Rapidly varied flow phenomenon in a two-layered flow, *J. Fluid Mech*. **47**, 241–256.

6. MacLatchy, M. and Lawrence, G: 2000, Investigation of radially spreading buoyant surface flows. In: *Proceedings*, *5th International Symposium on Stratified Flows*, University of British Columbia, Vancouver, Canada.
7. Tomasko, D.: 1993, An evaluation of dilution models for the discharge of produced water into the Gulf of Mexico, *Argone National Laboratories*.
8. Doneker, R.L. and Jirka, G.H.: 1990, *Expert System for Hydrodynamic Mixing Zone Analysis of Conventional and Toxic Submerged Single Port Discharges (CORMIX1)*, DeFrees Hydraulics Laboratory, Cornell University, EPA/600/3-90/012.
9. Ellison, T.H. and Turner, J.S.: 1959, Turbulent entrainment in stratified flows, *J. Fluid Mech.* **6**, 423–448.
10. U.S. Bureau of Reclamation: 1955 (June 1), *Research Studies on Stilling Basins, Energy Dissipation, and Associated Appurtenances*, Hydraulic Laboratory Report Hyd-399.
11. Benton, G.S.: 1954, The occurrence of critical flow and hydraulic jumps in a multi-layered fluuid system, *J. Meteorol*. **11**, 139–150.
12. Yih, C. and Guha, C.R.: 1955, Hydraulic jump in a fluid system of two layers, *Tellus* **7**, 358–366.
13. Rajaratnam, N. and Powley, R.L.: 1990, Hydraulic jumps in two layer flows, *Proceedings*, *Instn. Civ. Engrs.* **89**, 127–142.
14. Stefan, H. and Hayakawa, N.: 1972, Mixing induced by an internal hydraulic jump, *Water Resour. Bull.*, AWRA **8**, 531–545.
15. Chu, V.E. and Baddour, R.A.: 1984, Turbulent gravity stratified shear flows, *J. Fluid Mech.* **138**, 353–378.
16. Wright, S.J. and Kim, Y.: 1990, Density current propagation in flowing receiving fluid. In: *Proceedings*, *International Convference on Physical Modeling of Transport and Dispersion*, Massachusetts Institute of Technology, Massachusetts.
17. Armi, L.: 1986, The hydraulics of two flowing layers with different densities, *J. Fluid Mech.* **163**, 27–58.
18. Schijf, J.B. and Schönfeld, J.C.: 1953, Theoretical considerations on the motion of salt and fresh water. In: *Proceedings, Minnesota International Hydraulics Convention*, Minneapolis, Minnesota.
19. Jirka, G.H. and Harleman, D.R.F.: 1979, Stability and mixing of vertical plane buoyant jet in confined depth, *J. Fluid Mech.* **94**, 275–304.
20. Fischer, H.B., List, E.J., Koh, R.C.Y., Imberger, J. and Brooks, N.H.: 1979, *Mixing in Inland and Coastal Waters*, Academic Press.
21. Ulasir, M.: 2001, *Experimental and Numerical Study of Submerged, Round Buoyant Jets Impinging on a Horizontal Surface*, Thesis, University of Michigan.